Sol−Gel Preparation and Photoluminescence of Size Controlled Germanium Nanoparticles Embedded in a SiO₂ Matrix

Heqing Yang,*,†,‡ Xi Yao,§ Xingjun Wang,‡ Songhai Xie,# Yu Fang,† Shouxin Liu,† and Xiaoxiao Gu‡

School of Chemistry and Material Science, Shaanxi Normal University, Xi'an 710062, People's Republic of China, Surface Physics Laboratory, Fudan University, Shanghai 200433, People's Republic of China, Electronic Materials Research Laboratory, Xi'an Jiaotong University, Xi'an 710049, People's Republic of China, and Department of Chemistry, Fudan University, Shanghai 200433, People's Republic of China

Germanium nanoparticles of different sizes in silica glasses were prepared via a sol−gel method, using $Cl_3-Ge-C_2H_4-COOH$ and $Si(OC_2H_5)_4$ as the starting materials. The size of the germanium nanoparticles decreases as the heat-treatment time in a H_2 gas atmosphere increases, and, thus, the optical absorption edge shifts to higher energies. Silica gel glasses doped with germanium nanoparticles showed a strong room-temperature photoluminescence, with peaks at 570, 605, 676, and 730 nm. The peak position of the photoluminescence spectrum scarcely depends on the heat-treatment time. However, the photoluminescence intensity increases sharply as the heat-treatment time is reduced. The photoluminescence arises from germanium clusters <1−2 nm in diameter with a molecular character, instead of from nanocrystalline germanium with the diamond structure.

Introduction

In the past decade, a considerable amount of research has been devoted to the luminescence of group IV semiconductors of low dimensionality, to study quantum-confined electronic states and develop integrated optoelectronic devices directly on silicon. Much of this effort was inspired by the discovery of visible room-temperature photoluminescence (PL) in porous silicon that has been synthesized by an anodic etching of silicon.[1] Since then, many other methods for the synthesis of luminescent group IV nanocrystals have been reported. Nanocrystals embedded in a SiO₂ matrix offer an attractive option, because SiO₂ is a well-characterized material known to passivate semiconductor surfaces. For germanium, most reports of visible PL from low-dimensional structures have involved germanium nanocrystals embedded in SiO₂. Until now, a variety of methods have been used for the synthesis of germanium nanocrystals embedded in SiO₂, including co-sputtering of germanium and SiO₂,[2−4] Ge ion implantation,[5,6] atmospheric pressure chemical vapor deposition (APCVD),[7] and H₂ reduction of $Si_xGe_{1−x}O_2$,[8,9] etc. However, these methods require highly sophisticated equipment. In addition, sometimes it is not easy to find the conditions for reproducing samples that emit visible light.

The sol−gel method is attractive for glass preparation, because it provides unusual compositions at temperatures much lower than those required by the conventional melting technique. The sol−gel method has been used for the preparation of semiconductor microcrystallites of CdS, CuCl, CdTe, PbS, etc. dispersed in a SiO₂ glass.[10−13] Nogami et al.[14] first prepared germanium nanocrystals embedded in SiO₂ via the sol−gel process using $Si(OC_2H_5)_4$ (TEOS) and GeCl₄ as the starting materials and then observed visible PL from the germanium nanocrystals. However, until now, the preparation of germanium microcrystallites of controlled size via the sol−gel process has not been reported. We now present the preparation of germanium microcrystallites via a sol−gel process, using 3-trichlorogermanium propanoic acid ($Cl_3-Ge-C_2H_4-CO_2H$) as the germanium source. The sizes of the germanium nanoparticles can be easily controlled by changing the heating time in a H₂ gas atmosphere. The optical absorption, Raman, and PL spectra for germanium nanoparticles in SiO₂ are also investigated.

Experimental Section

Ge/SiO₂ gel glasses were prepared via the sol−gel method, using TEOS and $Cl_3-Ge-C_2H_4-COOH$ as the starting materials. TEOS was mixed with C_2H_5OH, H_2O, and a 2.0 M HCl solution. The molar ratio of TEOS:H₂O:C₂H₅OH was 1:2:1, and the HCl concentration was 0.01 M in the final mixture. After the mixture was stirred for 30 min, a solution of 0.5 M $Cl_3-Ge-C_2H_4-COOH$ in ethanol (the synthesis of $Cl_3-Ge-C_2H_4-COOH$ was described in the work of Bai et al.[15]) was added. The molar ratio of Ge:Si is 15:100. The mixture solution was stirred for 1 h at room temperature, then poured into a culture dish and left until it formed a stiff gel. This dried gel was heated in an air atmosphere for 10 h to 600 °C, at which temperature it was held for 10 h to form a GeO₂−SiO₂ gel glass. The gel glass was heated at 600 °C for a given time under a flowing (1.0 L/h) H₂ gas in a fused silica tube, in which the Ge⁴⁺ ion was reduced to form nanometer-sized germanium particles.

The germanium nanoparticles were characterized and analyzed by Raman spectra, high-resolution transmission electron microscopy (HRTEM) (JEOL model JEM 2011 HRTEM at 200 kV), and energy-dispersive X-ray spectroscopy (EDS). The

* Author to whom correspondence should be addressed. E-mail: HqYang@snnu.edu.cn.
† School of Chemistry and Material Science, Shaanxi Normal University.
‡ Surface Physics Laboratory, Fudan University.
§ Electronic Materials Research Laboratory, Xi'an Jiaotong University.
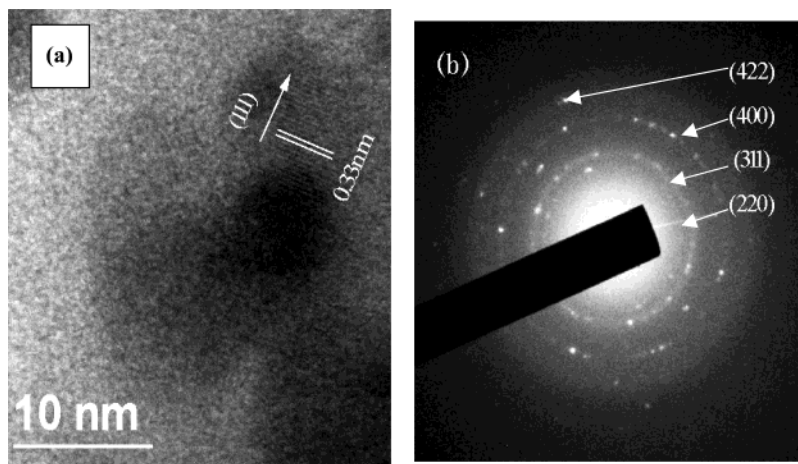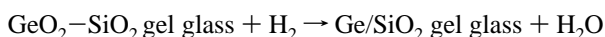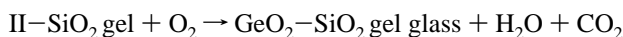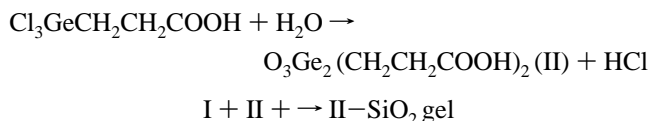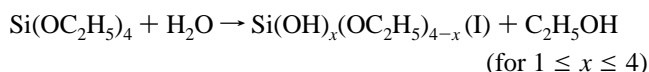# Department of Chemistry, Fudan University.

Figure 1. (a) High-resolution transmission electron microscopy (HRTEM) image and (b) electron diffraction pattern of $15Ge/100SiO_2$ gel glass heated at 600°C for 20 h in a H_2 gas atmosphere.

optical absorption measurements were performed with a spectrophotometer (Hitachi model U-2000). The Raman and PL spectra were measured using a micro-Raman setup (Renishaw model 2000) at room temperature. The 514.5-nm line from an Ar^+ laser was used as the incident light. The power density of the incident light on the sample surface was ~0.4 mW/μm^2 for Raman spectroscopy and 0.32×10^{-3} mW/μm^2 for PL spectroscopy.

Results and Discussion

The Ge/SiO_2 gel glass synthesized using this sol−gel method has a brown color. The extent of coloration increases as the heat-treatment time in a H_2 gas atmosphere increases. According to Nogami et al.,[14] in the reaction of a GeO_2-SiO_2 glass with H_2 gas, the Si^{4+} cation is much more stable than the Ge^{4+} cation and is not reduced by hydrogen in the temperature range of 400−800°C. The coloration of the GeO_2-SiO_2 gels is due to the reduction of Ge^{4+} cations in gel glasses. The reactions can be described as follows:

$$Si(OC_2H_5)_4 + H_2O \rightarrow Si(OH)_x(OC_2H_5)_{4-x}(I) + C_2H_5OH$$
$$(for\ 1 \leq x \leq 4)$$

$$Cl_3GeCH_2CH_2COOH + H_2O \rightarrow$$
$$O_3Ge_2(CH_2CH_2COOH)_2(II) + HCl$$

$$I + II + \rightarrow II-SiO_2\,gel$$

$$II-SiO_2\,gel + O_2 \rightarrow GeO_2-SiO_2\,gel\,glass + H_2O + CO_2$$

$$GeO_2-SiO_2\,gel\,glass + H_2 \rightarrow Ge/SiO_2\,gel\,glass + H_2O$$

To confirm the formation of germanium crystals, the $15Ge/100SiO_2$ gel glass heated for 20 h in a H_2 gas atmosphere was characterized by HRTEM, and the results are shown in Figure 1. Figure 1a shows a typical HRTEM image of the sample. The spacing of the crystallographic planes measured from the HRTEM image is ~0.33 nm, as indicated in Figure 1a. This spacing corresponds to the interplanar distance of the (111) lattice planes of germanium. We can observe cubic germanium nanocrystals with an ovoid shape and a size of 6 nm × 9 nm, dispersed in SiO_2 matrixes. Figure 1b shows the electron diffraction pattern, displaying four diffused rings. The rings are assigned to Ge(220), Ge(311), Ge(400), and Ge(422) diffraction lines. The electron diffraction pattern reveals that the nanoparticles are cubic germanium crystallites.
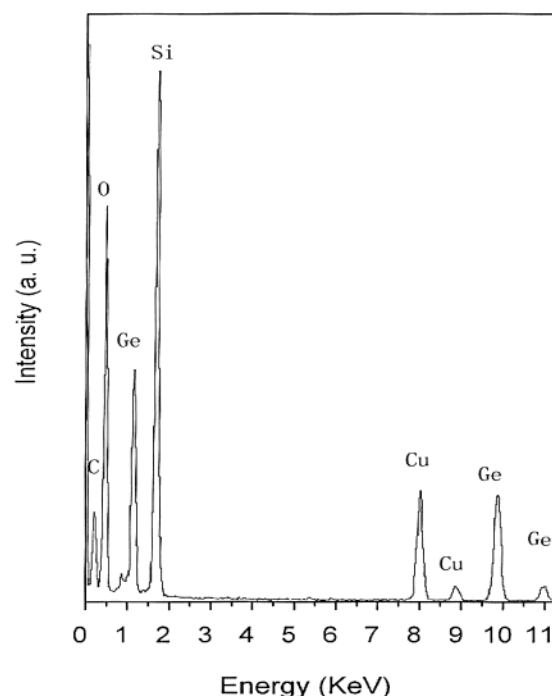

Figure 2. Energy-dispersive X-ray spectroscopy (EDS) spectrum of $15Ge/100SiO_2$ gel glass heated at 600°C for 20 h in a H_2 gas atmosphere.

An EDS facility attached to the HRTEM was used to analyze the chemical composition. The EDS data curve of the sample is depicted in Figure 2. The carbon- and copper-related peaks are due to the carbon contamination during the preparation of the TEM specimens and the presence of copper grids. Therefore, the gel glass consists of germanium, silicon, and oxygen. The molar ratio of Si:O:Ge was calculated 1:2.05:0.11.

Raman spectra of the gel glasses heated at 600°C for different times in a H_2 gas atmosphere were measured. The results are shown in Figure 3. Sharp scattering peaks at ~299 and 300 cm^{-1} are observed in the Raman spectra of $15Ge/100SiO_2$ gel glasses heated for 20 and 30 h in a H_2 gas atmosphere. The Raman band is attributed to the crystalline Ge−Ge phonon vibration mode, indicating the formation of germanium nanocrystallites. The gel glass heated for 10 h shows no evidence of the Ge−Ge phonon mode. The Raman spectrum of the gel glass heated for 0.5 h was not obtained, because the luminescence is so strong that the signal goes beyond the instrument
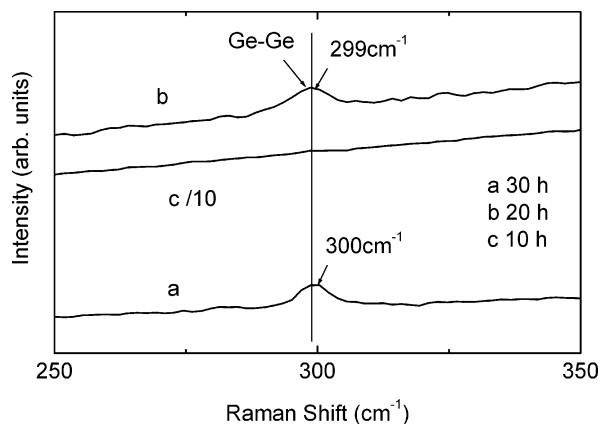
Size-Controlled Ge Nanoparticles in a SiO$_2$ Matrix

J. Phys. Chem. B, Vol. 107, No. 48, 2003 **13321**

Figure 3. Raman spectra of 15Ge/100SiO$_2$ gel glasses heated at 600°C for different times in a H$_2$ gas atmosphere.

Figure 4. Optical absorption spectra of 15Ge/100SiO$_2$ gel glasses heated at 600°C for different times in a H$_2$ gas atmosphere.

Figure 5. Photoluminescence (PL) spectra of 15Ge/100SiO$_2$ gel glasses heated at 600°C for different times in a H$_2$ gas atmosphere.

limit under the same conditions. As the heat-treatment time in a H$_2$ gas atmosphere is decreased, the growth time of germanium nanocrystals is decreased, and thus, the size of the germanium particles is reduced. The germanium nanoparticles precipitated may be so small that they could not form a complete crystal lattice when the heat-treatment time was <10 h, hence, no distinct Ge−Ge mode was observed from the Raman spectra. The peak breadth in Figure 3 was estimated from the full width at half-maximum (fwhm) and was observed to decrease as the time at temperature increased. A qualitative relationship between particle size and the peak breadth associated with the Ge−Ge phonon mode has been reported by Fujii et al.[16] The basis for this estimation of the average particle diameter comes from phonon localization within nanometer-sized crystallites, which results in a partial breakdown of the Raman selection rule, and hence, causes peak broadening. According to the method of Fujii et al., the average diameters of the germanium nanocrystals in samples heated for 20 and 30 h estimated from the fwhm values are 7.5 and 11 nm, respectively.

In the Raman spectra of bulk unstained germanium crystals, the Ge−Ge peak is symmetric and centered at 302 cm^{-1}.[17] Compared with bulk germanium, the Ge−Ge peaks of 15Ge/100SiO$_2$ gel glasses heated for 20 and 30 h all shift to lower frequencies by 2 and 3 cm^{-1}, respectively. We ascribe this downward shift to the competition between the compressive stress exerted upon the germanium nanocrystals and phonon confinement. The nearest-neighbor distance in SiO$_2$ is 0.16 nm, and that in germanium crystal is 0.24 nm. Therefore, the mismatch in the nearest-neighbor distance may lead to a compressive stress exerted upon the germanium nanocrystals, and, hence, an upward shift of the Raman peak occurs. The phonon confinement effect is the major factor in our samples; the downward shift of the Raman peaks caused by phonon confinement is partly compensated by the upward shift, because of the compressive stress. Therefore, a net downward shift is observed, compared to bulk germanium. The size of the germanium particles is reduced as the heat-treatment time in a H$_2$ gas atmosphere is decreased. Thus, the Ge−Ge peak of a sample heated for 20 h shifts to lower frequencies by 1 cm^{-1}, compared to that of a sample heated for 30 h.

Figure 4 shows the optical absorption spectra of the gel glasses heated at 600°C for different times in a H$_2$ gas atmosphere. The absorption edge is located at shorter wavelengths than that of bulk germanium (1867 nm, 0.664 eV),[18] and it becomes steeper and shifts toward longer wavelengths as the time of the reaction with H$_2$ gas is increased. The absorption is attributed to a transition from the highest hole sub-
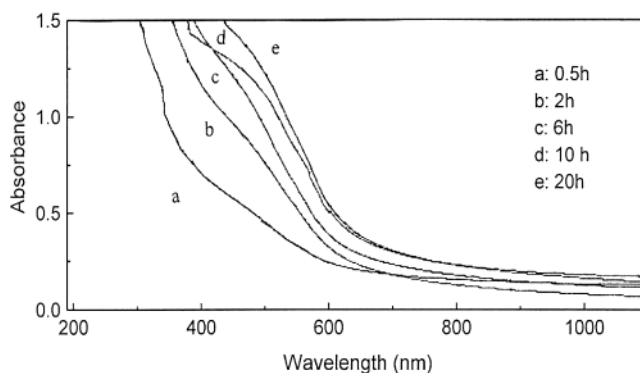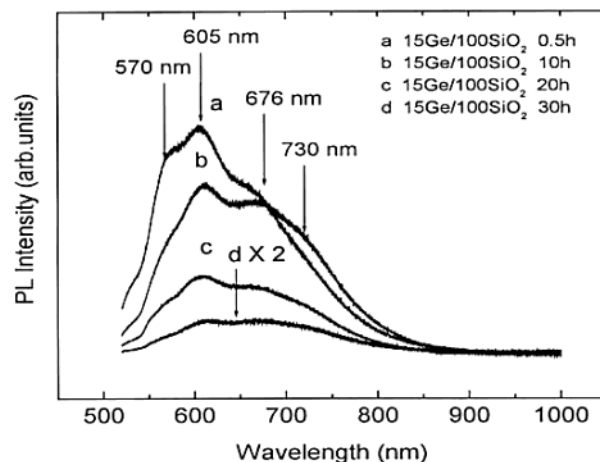
band level to the lowest electron sub-band level of a germanium nanoparticle. However, the absorption spectra show no well-resolved band structure but with a shoulder at a wavelength shorter than the absorption edge. This appears to be caused by the distribution of germanium particle sizes. The blue shift of the absorption edge can be explained on the basis of the quantum size effect of the carrier confinement. According to Efros and Efros,[19] the lowest excitation band gap (E_R) can be expressed as

$$E_R = E_g + \left(\frac{\hbar^2 \pi^2}{2R^2}\right)\left(\frac{1}{m_e} + \frac{1}{m_h}\right)$$

where E_g is the band gap for bulk crystal, m_e and m_h are the effective masses of the electron and hole, respectively, $\hbar$ is Planck's constant divided by 2π, and R is the radius of the particle. The energy increases as the size of the germanium nanoparticles decreases. The size of the germanium particles is reduced as the heating time is reduced. Hence, the optical absorption edge is located at shorter wavelengths than that of bulk germanium (1867 nm, 0.664 eV) and is shifted toward shorter wavelengths as the heating time is reduced.

PL spectra of the samples heated at 600°C for different times in a H$_2$ gas atmosphere at room temperature under the excitation of a 514.5-nm Ar$^+$ laser are shown in Figure 5. The sample heated for 0.5 h shows a strong and broad PL spectrum, ranging from 520 nm to 1000 nm, as shown by curve a in Figure 5. The broad PL spectrum is composed of fourfold peaks that overlap each other; the peak positions are located at 570, 605, 676, and 730 nm, respectively. A similar PL is observed from
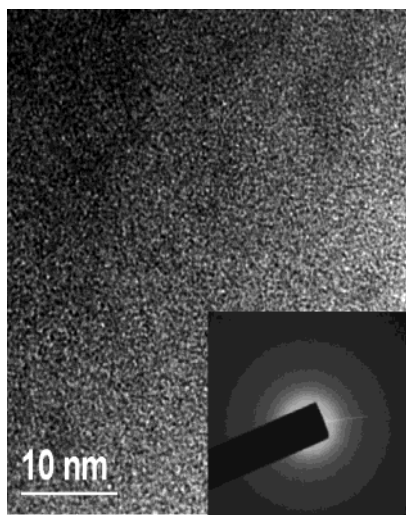
13322 *J. Phys. Chem. B, Vol. 107, No. 48, 2003*

Yang et al.

Figure 6. HRTEM image of 15Ge/100SiO$_2$ gel glass heated at 600°C for 0.5 h in a H$_2$ gas atmosphere.

the samples heated for 10, 20, and 30 h (curves b, c, and d, respectively). The peak positions of the PL spectra are almost the same for the four samples; however, the PL intensity decreases acutely as the heat-treatment time increases. The PL intensity ratio is 14:11:5:1 when the heat-treatment time is 0.5, 10, 20, and 30 h, respectively.

To confirm the origin of the PL presented in Figure 5, the PL spectrum of a pure SiO$_2$ gel heated at 600°C in an air atmosphere for 10 h was measured under the same conditions. The SiO$_2$ gel glass without germanium nanoparticles was observed to exhibit no PL. Therefore, the PL is, indeed, caused by the germanium nanoparticles embedded in SiO$_2$ gel glasses. In addition, the 15Ge/100SiO$_2$ gel glass heated for 0.5 h in a H$_2$ gas atmosphere was characterized by HRTEM, and the results are shown in Figure 6. No distinct nanoparticles were observed in HRTEM image of the sample, and the electron diffraction pattern (inset) displays a typical amorphous diffraction ring. The electron diffraction pattern reveals that germanium is present as an amorphous structure in the sample that exhibits the strongest PL. This is also supported by the Raman spectra. These data suggest that the germanium may be dispersed as ultrasmall germanium particles with a molecular character instead of nanocrystalline germanium with a diamond structure in SiO$_2$ matrixes. The size of the germanium clusters is estimated to be <1−2 nm. The germanium clusters <1−2 nm in diameter with molecular character embedded in SiO$_2$ glassy matrix may cause the PL. When the heat-treatment time in a H$_2$ gas atmosphere is increased to 20 and 30 h, the majority of germanium is present as nanocrystalline germanium with the diamond structure in SiO$_2$ matrixes. Thus, the concentration of the ultrasmall germanium particles with a molecular character decreases, and, thus, the PL intensity decreases.

Takeoka et al.[20,21] reported size-dependent PL from germanium nanocrystals with an average diameter of 0.9−5.3 nm in the near-IR region (1.54−0.88 eV, 805−1409 nm). However, many authors have reported that germanium nanocrystal−SiO$_2$ films prepared by co-sputtering of germanium and SiO$_2$,[22] H$_2$ reduction of Si$_{1−x}$Ge$_x$O$_2$ alloy,[8] and APCVD[7] exhibit strong visible PL at ~2.2 eV (564 nm), independent of the size of the

germanium nanocrystals (2−15 nm), and considered that PL results from germanium crystals with a critical size (diameter) of 4−5 nm or less. In this work, strong room-temperature PL with peaks at 570, 605, 676, and 730 nm was observed from the germanium nanoparticles in SiO$_2$ gel glasses. When the heat-treatment time is 0.5 h, the germanium is present as germanium clusters <1−2 nm in diameter with molecular character, instead of cubic germanium nanocrystals in SiO$_2$ gel glasses, and the strongest PL is observed. Therefore, the PL results from the ultrasmall molecular-like germanium nanoparticles, instead of nanocrystalline germanium with the diamond structure.

In conclusion, germanium nanocrystals embedded in bulk SiO$_2$ glasses were prepared by combining the sol−gel process and the heat treatment in H$_2$ gas. The size of the germanium nanoparticles decreases as the heat-treatment time in a H$_2$ gas atmosphere decreases, and, thus, the optical absorption edge shifts to higher energies. Silica gel glasses doped with germanium nanoparticles showed strong room-temperature photoluminescence (PL), with peaks at 570, 605, 676, and 730 nm. The PL results from germanium clusters <1−2 nm in diameter with molecular character, instead of cubic germanium nanocrystals.

References and Notes

(1) Canham, L. T. *Appl. Phys. Lett*. **1990**, *57*, 1046.
(2) Maeda, Y.; Tsukamoto, N.; Yazawa, Y.; Kanemitsu, Y.; Masumoto, Y. *Appl. Phys. Lett*. **1991**, *59*, 3168.
(3) Okamoto, S.; Kanemitsu, Y. *Phys. Rev. B* **1996**, *54*, 16421.
(4) Yue, L. P.; He, Y. Z. *J. Appl. Phys*. **1997**, *81*, 2910.
(5) Wu, X. L.; Gao, T.; Bao, X. M.; Yan, F.; Jiang, S. S.; Feng, D. *J. Appl. Phys*. **1997**, *82*, 2704.
(6) Masuda, K.; Yamamoto, M.; Kanaya, M.; Kanemitsu, Y. *J. Non-Cryst. Solids* **2002**, *299−302*, 1097.
(7) Dutta, A. K. *Appl. Phys. Lett*. **1996**, *68*, 1189.
(8) Paine, D. C.; Caragianis, C.; Kim, T. Y.; Shigesato, Y.; Ishahara, T. *Appl. Phys. Lett*. **1993,** *62*, 2842.
(9) Liu, W. S.; Chen, J. S.; Nicolet, M. A.; Arbet-Engels, V.; Wang, K. L. *Appl. Phys. Lett*. **1993**, *62*, 3321.
(10) Nogami, M.; Nagaska, K.; Kato, E. *J. Am. Ceram. Soc*. **1990,** *73*, 2097.
(11) Nogami, M.; Zhu, Y. Q.; Tohyama, Y.; Nagasaka, K.; Tokizaki, T.; Nakamura, A. *J. Am. Ceram. Soc*. **1991**, *74*, 238.
(12) Nogami, M.; Nagasaka, K.; Suzuki, T. *J. Am. Ceram. Soc*. **1992**, *75*, 220.
(13) Yao, L. Z.; Ye, C. H.; Mo, C. M.; Cai, W. L.; Zhang, L. D. *J. Cryst. Growth* **2000**, *216*, 147.
(14) Nogami, M.; Abe, Y. *Appl. Phys. Lett*. **1994**, *65*, 2545.
(15) Bai, M. Z.; Yang, S. J.; Sun, L. J.; Wang, S. X. *Chin. J. Org. Chem*. **1987**, *7*, 85.
(16) Fujii, M.; Hayashi, S.; Yamamoto, K. *Appl. Phys. Lett*. **1990**, *57*, 2692.
(17) Hellwege, K. H. *Landolt−Bornstein Numerical Data and Functional Relationships in Science and Technology*. Springer−Verlag: Berlin, Heidelberg, New York, 1982; Vol. 17, Subvol. a, p 115.
(18) Hellwege, K. H. *Landolt−Bornstein Numerical Data and Functional Relationships in Science and Technology*. Springer−Verlag: Berlin, Heidelberg, New York, 1982; Vol. 17, Subvol. a, p 87.
(19) Efros, Al. L.; Efros, A. L. *Sov. Phys. Semicond*. **1982**, *16*, 772.
(20) Takeoka, S.; Fujii, M.; Hayashi, S.; Yamamoto, K. *Phys. Rev. B* **1998**, *58*, 7921.
(21) Takeoka, S.; Fujii, M.; Hayashi, S.; Yamamoto, K. *Appl. Phys. Lett*. **1999**, *74*, 1558.
(22) Kanemitsu, Y.; Uto, H.; Masumoto, Y.; Maeda, Y. *Appl. Phys. Lett*. **1992**, *61*, 2187.